PHYSICAL PROPERTIES OF SOME UNEQUILIBRATED ANTARCTIC ORDINARY CHONDRITES

Kiyoshi YOMOGIDA and Takafumi MATSUI

Geophysical Institute, Faculty of Science, University of Tokyo, 11–16, Yayoi 2-chome, Bunkyo-ku, Tokyo 113

Abstract: The intrinsic and bulk densities, porosity, thermal diffusivity, and ultrasonic-wave velocities (V_p and V_s) were measured for four unequilibrated ordinary chondrites (Y-74156, -74191, -74647 and -75097). Thermal diffusivity was also measured for five equilibrated ordinary chondrites (ALH-77288, -77294, -78103, -78251 and MET-78003). V_p and V_s measurements were made for three mutually perpendicular directions at room temperature and one atmosphere pressure. Thermal diffusivity was measured under vacuum conditions (below 10^{-3} mmHg) in the temperature range of 100 to 500 K. V_p and V_s values are much smaller than those expected from their mineral compositions. The decrease in V_p and V_s is much greater than that estimated from the porosity value itself. It is suggested that many oblate pores, *i.e.* cracks, exist in the samples. Aspect ratio of cracks is estimated to be much smaller than 0.05. Such thin cracks are presumably produced by impact events, although we cannot observe any heavy shock induced features in thin sections. Velocity anisotropy between transmitting directions is observed in almost all samples. Thermal diffusivities are also much smaller than those expected from their mineral compositions. Existence of many cracks is also suggested from the thermal diffusivity-porosity relations. Relationship between the measured physical properties and the petrologic types was investigated. For H chondrites we can see a rough trend that porosity decreases with increase in petrologic type number. For L chondrites, however, we cannot see any clear correlation between the physical properties and the petrologic types.

1. Introduction

As mentioned in previous papers (MATSUI and OSAKO, 1979; MATSUI *et al.*, 1980; YOMOGIDA and MATSUI, 1981), the physical properties of chondrites are expected to contain some information on the origin and formation processes of their parent bodies. Therefore, systematic measurements of physical properties are required. For several years we have measured physical properties mostly of the equilibrated oridinary chondrites. In this paper we present intrinsic and bulk densities, porosity, ultrasonic-wave velocities, and thermal diffusivity of the unequilibrated ordinary chondrites and thermal diffusivity of the equilibrated ones.

2. Sample Descriptions

The newly distributed four samples (Yamato-74156, -74191, -74647 and -75097) are all classified as unequilibrated ordinary chondrites (YANAI, 1979). They are fresh

but we can see several tiny cracks on their surfaces. Existence of a few tiny cracks does not affect the physical properties significantly. We prepared the samples as nearly rectangular parallelepipeds by cutting and grinding. Sample descriptions of the four samples are summarized in Table 1. In addition to these samples, we measured the thermal diffusivity of ALH-77288, -77294, -78103, -78251 and MET-78003. Sample descriptions of these are given in Table 2.

Table 1. Intrinsic and bulk densities and porosity.

Sample	Type	Volume (cm^3)	Mass (g)	Density (g/cm^3)		Porosity (%)
				Bulk	Intrinsic	
Y-74156	H4	4.05	13.98	3.45	3.80	9.2
Y-74191	L3	2.39	7.72	3.23	3.60	10.3
Y-74647	H4–5	2.63	9.17	3.49	3.83	9.1
Y-75097	L4	2.40	7.85	3.28	3.65	10.3

Table 2. Sample description for thermal diffusivity measurements.

Sample	Type	Porosity (%)	Size (mm)	Mass (g)
Y-74156	H4	9.2	3.64×3.75×3.81	0.179
Y-74191	L3	10.3	3.50×3.69×3.73	0.155
Y-74647	H4–5	9.1	3.66×3.68×3.68	0.171
Y-75097	L4	10.3	3.47×3.58×3.62	0.146
ALH-77288	H6	2.0	3.48×3.49×3.59	0.163
ALH-77294	H5	12.9	3.55×3.57×3.58	0.150
ALH-78103	L6	13.4	3.40×3.45×3.51	0.132
ALH-78251	L6	13.2	3.21×3.45×3.46	0.120
MET-78003	L6	7.8	3.21×3.41×3.45	0.127

In the following we give brief petrographic descriptions of the unequilibrated samples (NAGAHARA, private communication). The petrographic features of Yamato-74191 are almost the same as those reported in detail by IKEDA and TAKEDA (1979) and KIMURA *et al.* (1979), and are not mentioned here.

2.1. Yamato-74156

The section shows well-developed chondritic texture with various kinds of chondrules. Groundmass of chondrules is cryptocrystalline or devitrified glass. Matrix is weakly crystallized and transparent. Olivine is euhedral or subhedral and pyroxene is polysynthetically twinned clinoenstatite. No clear opaque shock veins can be seen.

2.2. Yamato-74647

The section consists mainly of olivine with minor amounts of orthopyroxene and plagioclase. There remain cryptocrystalline materials and chondrules with barred olivine or radial pyroxene. Chondritic structure is moderately developed but chondrules tend to merge with the granular groundmass. Some opaque shock veins can be seen. Degree of shock would be low, because plagioclase did not transform into maskelynite. These characteristics are consistent with the description reported by KIMURA *et al.* (1978).

2.3. Yamato-75097

The outline and internal structure of chondrules have almost become diffuse. The matrix and the groundmass of chondrules are also well-recrystallized. The section consists mainly of anhedral olivine and well-crystallized plagioclase grains about 100 μm long, and of a minor amount of orthopyroxene. Some large whitlockite or apatite grains about 400 μm long can be seen. There are some opaque shock veins but plagioclase did not transform into maskelynite.

3. Experimental Techniques

The intrinsic density, ρ_0, was measured by using the helium-pycnometer. The accuracy of measurements was within 2% (YOMOGIDA and MATSUI, 1981). The bulk density, ρ_{bulk}, was simply calculated from the mass and the volume of samples. The error of measurements was less than 1%. The porosity, ϕ, was calculated from $\phi=1-\rho_{bulk}/\rho_0$. Elastic wave velocities (V_p and V_s) were measured for three mutually perpendicular directions by employing the pulse transmission method under one atmosphere pressure and at room temperature. Either 1 or 2 MHz PZTs were used for V_p measurements. 2 MHz PZTs were used for V_s measurements. No detectable changes in velocity values with change in the frequency of transducers could be observed. The accuracy of V_p determination was better than a few %. On the other hand, the onset point of shear wave was blurred and thus it was very difficult to determine the onset point precisely. Therefore, accuracy of the determination of V_s values might not be better than 10%. Thermal diffusivity was measured by the modified Angstrom method in vacuum (below 10^{-3} mmHg) and at the temperature range of 100 to 500 K (MATSUI and OSAKO, 1979). Accuracy of the measurements is estimated to be better than 10%.

4. Results and Discussions

4.1. Density and porosity

The intrinsic and bulk densities and porosity of the four unequilibrated samples are summarized in Table 1. The intrinsic densities are almost identical with the theoret-

Table 3. Standard mineral compositions and physical properties of H and L chondrites.

	H	L
Mineral composition (wt%)		
Olivine	37 ($Fo_{80}Fa_{20}$)	49 ($Fo_{75}Fa_{25}$)
Orthopyroxene	25 ($En_{83}Fs_{17}$)	23 ($En_{78}Fs_{22}$)
Clinopyroxene	5 ($En_{49}Fs_6Wo_{45}$)	6 ($En_{48}Fs_8Wo_{44}$)
Plagioclase	8 ($Or_6An_{12}Ab_{82}$)	8 ($Or_6An_{10}Ab_{84}$)
Troilite	5	5
Fe-Ni metal	20 (Fe: Ni=11: 1)	9 (Fe: Ni=7: 1)
Physical properties		
ρ_0 (g/cm^3)	3.81	3.61
V_p (km/s)	7.61	7.80
V_s (km/s)	4.45	4.58
κ at 300 K (10^{-7} m^2/s)	17.0	15.6
C_p at 300 K (10^3J/kg/K)	.724	.758

ical values calculated from assumed mineral compositions of the standard ordinary chondrites (see Table 3). The intrinsic density of H chondrites is larger than that of L chondrites because of the higher content of Fe-Ni metal. As a matter of course, the intrinsic density of ordinary chondrites is much larger than that of terrestrial rocks (for example, 2.7–2.8 g/cm^3 for sedimentary rocks and 3.3–3.4 g/cm^3 for ultramafic rocks). The porosity values of the unequilibrated ordinary chondrites are about 10%. These are larger than the porosities of many igneous rocks (less than 5%) but smaller than those of usual sedimentary rocks (as large as 20%).

The porosity of the aggregated powder compacted by shaking and tapping is known to be larger than 30%. The porosity values of the unequilibrated chondrites are much lower than this value. This suggests that some sort of physical process to reduce the porosity of chondrites has operated during their consolidation.

4.2. Elastic-wave velocity

The results of the ultrasonic-wave velocity measurements are summarized in Table 4. As clearly seen in this table, velocity anisotropy exists between transmitting directions for each sample.

Table 4. Elastic-wave velocity.

Sample	Direction	Length (mm)	Velocity V_p(km/s)	Velocity V_s(km/s)
Y-74156	L1	14.98	3.23	1.87
	L2	15.76	3.38	1.77
	L3	17.16	3.29	2.01
Y-74191	L1	11.08	3.36	1.97
	L2	13.76	3.74	2.08
	L3	15.65	3.38	2.05
Y-74647	L1	12.03	2.74	1.65
	L2	14.45	3.09	1.92
	L3	15.14	2.98	1.87
Y-75097	L1	12.73	2.64	1.68
	L2	12.77	2.29	1.49
	L3	14.74	2.90	1.54

The elastic-wave velocities are influenced not only by the mineral composition but also by amount and shape of the pores. If the samples contain no pores or cracks, the theoretical V_p values are calculated to be about 7.6 km/s for the H chondrite and 7.8 km/s for the L chondrite, respectively, from their mineral compositions (see Table 3). The measured values were much smaller than the theoretical values. This feature was also noticed in the previous V_p measurements (YOMOGIDA and MATSUI, 1981). The mean compressional-wave velocities are plotted against the porosity in Fig. 1. Data of the previous measurements are also included in this figure. It is clear that the V_p decreases with increase in porosity. The degree of decrease in V_p is dependent not only on the porosity but also on the shape distribution of pores. The effect of oblated pores (cracks) on the elastic constants has been studied by many authors. O'CONNEL and BUDIANSKY (1974) considered very thin ellipsoidal cracks with random orientation and investigated the effect of the aspect ratio of cracks, $\alpha=c/a$, on elastic constants, where a

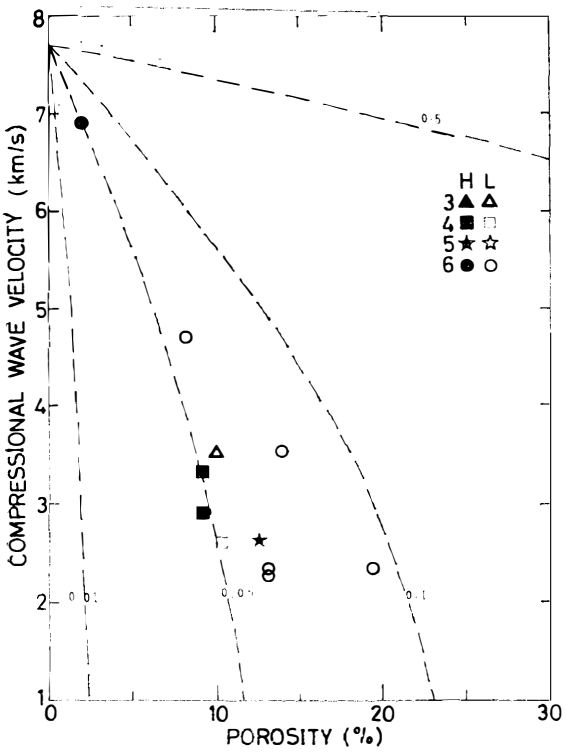

Fig. 1. Mean compressional-wave velocity, V_p, vs. porosity, ϕ, systematics. The broken lines are the theoretical relations derived by assuming that all the pores have the same mean aspect ratio. The numbers indicate mean aspect ratios of pores. (Y-74647 is classified into H4–5 but plotted as H4 in this figure.)

and c are lengths of the long and short axes. They gave the following expressions for porosity (ϕ), Poisson's ratio (ν), bulk modulus (Y), and rigidity (μ), respectively:

$$\phi = 4\pi/3\langle\alpha\rangle\varepsilon,$$

$$\bar{\nu} \sim \nu(1-16\varepsilon/9),$$

$$\bar{Y}/Y = 1-16\varepsilon/9(1-\bar{\nu}^2)/(1-2\bar{\nu}), \quad \text{and}$$

$$\bar{\mu}/\mu = 1-32\varepsilon/45(1-\bar{\nu})(5-\bar{\nu})/(2-\bar{\nu}),$$

where ε is crack density parameter. Symbols with a head bar represent effective values. Using these expressions, we can calculate a degree of decrease in V_p as a function of the porosity and aspect ratio. It is assumed that all the pores have common aspect ratio. The theoretical curves thus derived are shown by the broken lines in Fig. 1. Numbers attached to the lines designate the mean aspect ratio, $\langle\alpha\rangle$. It is clear from this figure that decrease in V_p with increase in porosity is much larger than that calculated by assuming that all the pores have spherical shape. Data are distributed between the curves for aspect ratios of 0.05 and 0.1. The assumption of homogeneity for the aspect ratio is not true and it gives an overestimated aspect ratio, because the porosity value depends on the density of spherical pores rather than that of oblated ones whereas the decrease in V_p depends inversely. It is therefore inferred that the ordinary chondrites contain thin cracks with aspect ratio much lower than 0.05. Such thin cracks presumably originate by impact events. Although no clear features due to heavy impact events can be observed in most thin sections, the V_p-ϕ relation suggests that ordinary chondrites may have experienced multiple impact histories like the lunar rocks. It is also interesting to note that decrease in V_p for H chondrites is rather large compared

with that for L chondrites.

The isotropic elastic constants calculated from the mean V_p, V_s and ρ_{bulk} are summarized in Table 5.

Table 5. Elastic properties of unequilibrated ordinary chondrites.

Sample	Type	ρ_{bulk} (g/cm^3)	ρ_0 (g/cm^3)	ϕ (%)	V_p (km/s)	V_s (km/s)	λ (kbar)	μ (kbar)	Y (kbar)	E (kbar)	ν
Y-74156	H4	3.45	3.80	9.2	3.30	1.88	132	122	213	308	0.26
Y-74191	L3	3.23	3.60	10.3	3.49	2.03	127	134	216	332	0.24
Y-74647	H4–5	3.49	3.83	9.1	2.93	1.81	70.8	115	147	273	0.19
Y-75097	L4	3.28	3.65	10.3	2.61	1.57	61.8	80.6	116	196	0.22

4.3. Thermal diffusivity

The thermal diffusivity shows a fairly large temperature dependency. Thermal diffusivity is plotted against the reciprocal of absolute temperature in Fig. 2. We can see a linear relationship between these quantities. The data were fitted to the empirical formula, $\kappa=A+B/T$, to obtain smoothed values, where κ is the thermal diffusivity and T is the absolute temperature. We have used the formula, $\kappa=A+B/T+CT^3$ in the previous papers. The term CT^3 is a contribution of the heat transfer by radiational mode. The radiational mode is, however, negligible in the temperature range below 500 K, compared with other modes such as lattice vibration. Such a situation is clearly seen in Fig. 2. Therefore, we employed $\kappa=A+B/T$ in this study, instead of $\kappa=A+B/T+CT^3$. Coefficients were determined by least-square fitting and are tabulated in

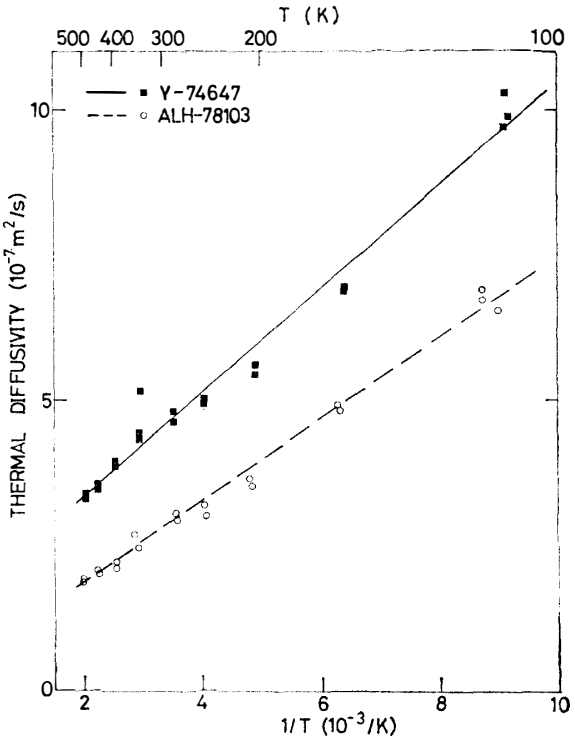

Fig. 2. Thermal diffusivity, κ, vs. reciprocal of temperature, $1/T$, for Yamato-74647 and ALH-78103. The solid and broken lines are derived by least-square fitting.

Table 6. Coefficients A and B of the empirical equation for thermal diffusivity ($\kappa=A+B/T$).

Sample	A ($10^{-7}m^2s^{-1}$)	B ($10^{-4}m^2s^{-1}K$)
Y-74156	2.35±0.23	1.16 ±0.048
Y-74191	2.65±0.25	0.818±0.050
Y-74647	1.59±0.19	0.888±0.037
Y-75097	1.19±0.20	0.803±0.042
ALH-77288	−1.64±2.14	3.82 ×0.49
ALH-77294	−0.30±0.16	0.871±0.034
ALH-78103	0.48±0.08	0.699±0.017
ALH-78251	−0.49±0.14	1.03 ±0.030
MET-78003	2.49±0.51	1.13 ±0.10

Table 7. Thermal diffusivity, $\kappa(10^{-7}m^2s^{-1})$, of antarctic ordinary chondrites.

Sample	Temperature (K)								
	100	150	200	250	300	350	400	450	500
Y-74156	13.9	10.1	8.13	6.97	6.20	5.65	5.24	4.92	4.66
Y-74191	10.8	8.11	6.75	5.93	5.38	4.99	4.70	4.47	4.29
Y-74647	10.5	7.51	6.03	5.14	4.55	4.13	3.81	3.56	3.37
Y-75097	9.22	6.54	5.20	4.40	3.86	3.48	3.19	2.97	2.79
ALH-77288	36.5	23.8	17.5	13.6	11.1	9.27	7.91	6.85	6.00
ALH-77294	8.41	5.51	4.06	3.19	2.61	2.19	1.88	1.64	1.44
ALH-78103	7.47	5.14	3.97	3.27	2.81	2.47	2.22	2.03	1.87
ALH-78251	9.81	6.38	4.66	3.63	2.94	2.45	2.09	1.80	1.57
MET-78003	13.8	10.0	8.15	7.01	6.26	5.72	5.32	5.00	4.75

Table 6. The smoothed diffusivity values are given in Table 7 and shown in Fig. 3 by the solid and broken lines. Thermal diffusivities of ALH-77288 are rather scattered. This is due to a high thermal diffusivity of ALH-77288. High thermal diffusivity of ALH-77288 is ascribed to its low porosity (see Table 2). When the sample length is the same as that of other samples, we have to use thermal waves with very short periods for measurements of the sample with high thermal diffusivity. Unfortunately, we did not expect such a high thermal diffusivity of ALH-77288 before sample preparation. Therefore, the length of ALH-77288 was almost the same as that of other samples. We had to use the period of 10 s for the measurement of ALH-77288 in the lowest temperature. In this case the amplitude of the thermal wave is so small that we could not determine amplitude and phase shift precisely.

For the ordinary chondrites without any pores or cracks, the thermal diffusivity at 300 K is calculated to be 17.0 m^2/s for the H chondrite and 15.6 m^2/s for the L chondrite from their mineral compositions (see Table 3). The measured values are much lower than these theoretical values, except for ALH-77288. Thermal diffusivity is influenced significantly by both the pore volume and the shape distribution of pores. The effect of the shape of pores on thermal conductivity was investigated by WALSH and DECKER (1966). They gave the following expressions for the effect of the mean aspect ratio of cracks on the thermal conductivity.

$$(K_s-K_v)/K_s=2\phi/3\pi\langle\alpha\rangle,$$

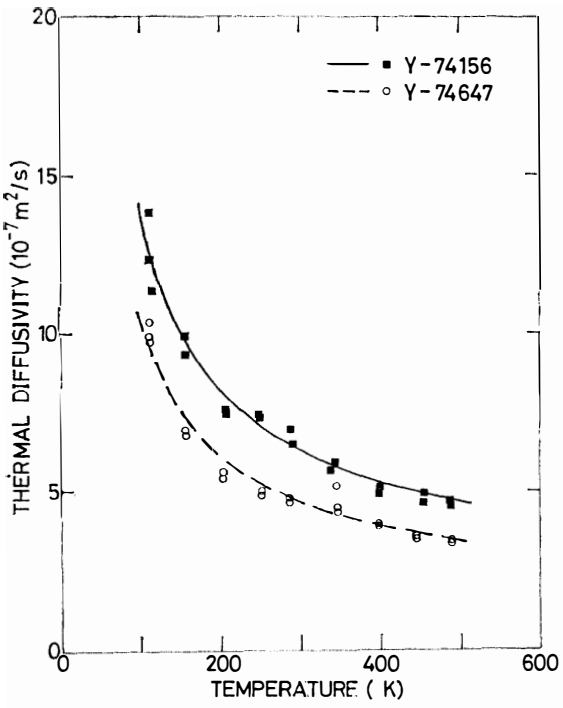

Fig. 3a.

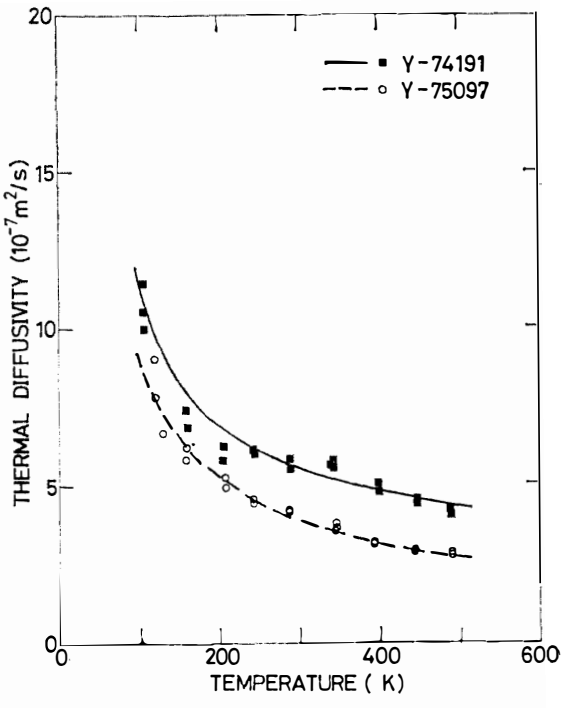

Fig. 3b.

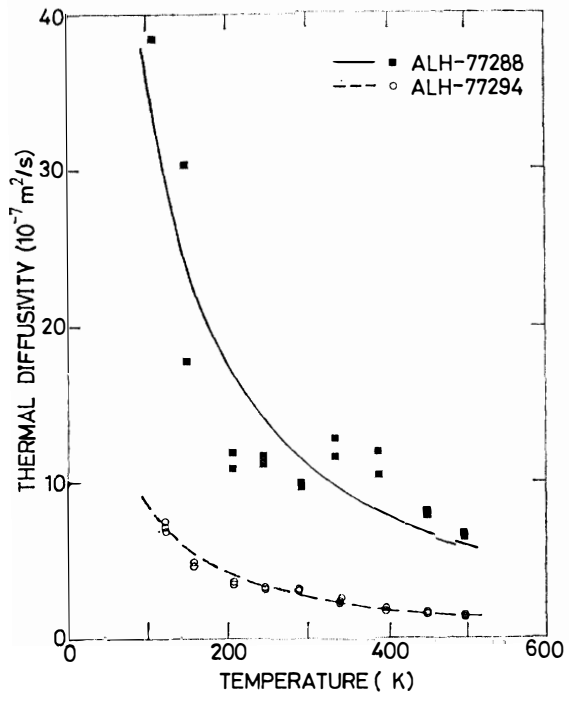

Fig. 3c.

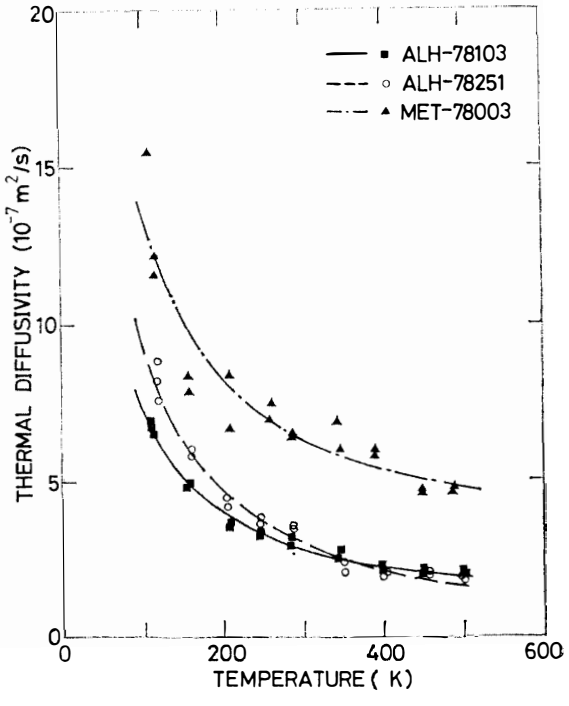

Fig. 3d.

Fig. 3. Thermal diffusivity, κ, vs. temperature, T, for (a) Yamato-74156 and -74647, (b) Yamato-74191 and -75097, (c) ALH-77288 and -77294 and (d) ALH-78103, -78251 and MET-78003.

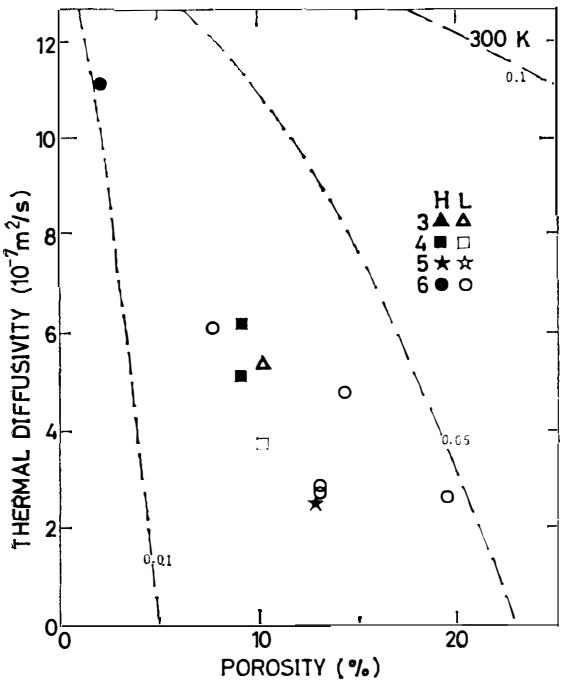

Fig. 4. Thermal diffusivity, κ, vs. porosity, ϕ, systematics. The broken lines are the theoretical relations derived by assuming that all the pores have the same mean aspect ratio. The numbers indicate mean aspect ratios of pores. (Y-74647 is classified into H4–5 but plotted as H4 in this figure.)

where K_v and K_s are the effective thermal conductivity in vacuum and the thermal conductivity calculated from mineral composition and ϕ and $\langle\alpha\rangle$ are porosity and mean aspect ratio of pores, respectively. Thermal conductivity, K, is related to thermal diffusivity by $K=\rho_{\mathrm{bulk}}C_p\kappa$, where C_p is the specific heat. C_p is calculated from mineral compositions (see Table 3). Using above expressions, we can estimate the mean aspect ratio of pores in the sample. It is assumed in this calculation that aspect ratios of the pores are all the same. The thermal diffusivity at 300 K is plotted against the porosity in Fig. 4. Theoretical curves as functions of $\langle\alpha\rangle$ are shown by broken lines. The data are distributed between the theoretical curves for the mean aspect ratio of 0.01 and 0.05. This is consistent with the result derived from elastic-wave velocity versus porosity diagram. This also suggests that the ordinary chondrites contain many cracks in addition to the nearly spherical pores. The mean aspect ratio obtained from κ *vs.* ϕ diagram is rather smaller than that from V_p *vs.* ϕ diagram. It is, however, uncertain that such a difference is meaningful.

4.4. Porosity vs. petrologic-type relations

It is shown in the previous sections that elastic-wave velocities and thermal diffusivities are well correlated with porosity. In this section, we investigate the relations between petrologic types and porosity. The reason why we take up the porosity as a typical physical property is that porosity seems to have been less influenced by the secondary effects such as impact events and weathering. As shown in the previous sections, other properties such as elastic-wave velocity and thermal diffusivity are influenced significantly by the shape and volume of cracks that are likely to be caused by secondary effects. In Fig. 5 we plot the porosity of eleven antarctic chondrites measured so far and that of ten non-antarctic chondrites reported by other reseachers (ALEXEYEVA, 1958, 1960; STACEY *et al.*, 1961) against the petrologic type. For H chondrites we can

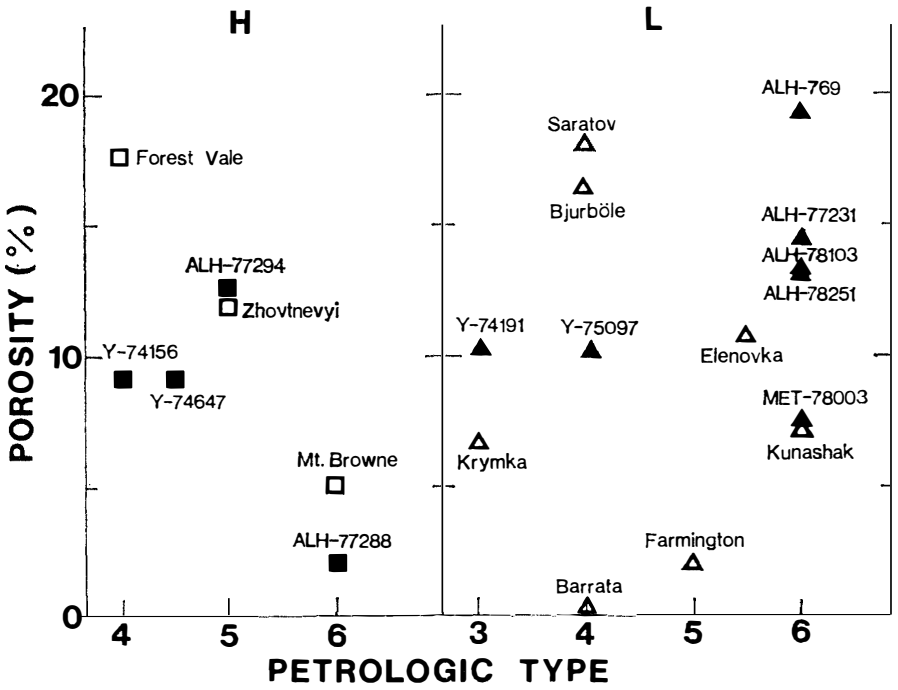

Fig. 5. Porosity vs. petrologic-type systematics. ▲ and ■ represent the data measured by our group, while △ and □ represent the data reported by ALEXEYEVA *(1958, 1960) and* STACEY *et al. (1961).*

see an overall trend that the porosity decreases with increase in the number of the petrologic type, although it is not well defined. However, for L chondrites such a correlation cannot be found. On the contrary, most of the L6 chondrites have higher porosity values than the unequilibrated ones.

As mentioned in the Subsection 4.1, some sort of physical process to reduce the porosity of chondrites has operated in ordinary chondrites. If sintering is a dominant process to decrease an amount of pores, the degree of consolidation is expected to increase with the maximum temperature which the chondrites have experienced, because sintering depends significantly on temperature, compared with other factors. The petrologic type is considered to represent a measure of the maximum metamorphic temperature. If so, the above result may indicate that for L chondrites sintering has not developed during the stage in which the observed metamorphic textures have been acquired.

5. Conclusions

We have measured the physical properties of eleven antarctic ordinary chondrites of various types to date. Chondrites contain Fe-Ni metal, so that we can see a clear difference in the intrinsic density between H and L chondrites. Elastic-wave velocities and thermal diffusivity are related to porosity and shape distribution of pores. It is inferred from V_p *vs.* ϕ diagram that ordinary chondrites contain many cracks in addition to the nearly spherical pores. These cracks are thought to have been produced by impact events. We can see a rough trend that the porosity of the H chondrites de-

creases with increase in petrologic type number. However, such a correlation cannot be observed for the L chondrites. This means that the consolidation stage of L chondrites may not be related to the metamorphic stage.

Acknowledgments

The authors wish to express their sincere thanks to Prof. T. NAGATA for his permission to use the meteorite samples for this work. They are also very much indebted to Ms. H. NAGAHARA for the petrographic description of our samples and to Drs. K. KURITA and Y. HAMANO for their great advice in the measurements.

References

ALEXEYEVA, K. N. (1958): Physical properties of stony meteorites and their interpretation based on the hypothesis on the origin of meteorites. Meteoritika, **16**, 67–77.

ALEXEYEVA, K. N. (1960): New data on physical properties of stony meteorites. Meteoritika, **18**, 68–76.

IKEDA, Y. and TAKEDA, H. (1979): Petrology of the Yamato-74191 chondrite. Mem. Natl Inst. Polar Res., Spec. Issue, **12**, 38–58.

KIMURA, M., YAGI, K. and OBA, Y. (1978): Petrological studies of Yamato-74 meteorites (2). Mem. Natl Inst. Polar Res., Spec. Issue, **8**, 156–169.

KIMURA, M., YAGI, K. and ONUMA, K. (1979): Petrological studies on chondrules in Yamato-74 meteorites. Mem. Natl Inst. Polar Res., Spec. Issue, **12**, 114–133.

MATSUI, T. and OSAKO, M. (1979): Thermal property measurement of Yamato meteorites. Mem. Natl Inst. Polar Res., Spec. Issue, **15**, 243–252.

MATSUI, T., HAMANO, Y. and HONDA, M. (1980): Porosity and compressional-wave velocity measurement of antarctic meteorites. Mem. Natl Inst. Polar Res., Spec. Issue, **17**, 268–275.

O'CONNEL, R. J. and BUDIANSKY, B. (1974): Seismic velocities in dry and saturated cracked solids. J. Geophys. Res., **79**, 5412–5426.

STACEY, F. D., LOVERING, J. F. and PARRAY, J. G. (1961): Thermomagnetic properties, natural magnetic moments, and magnetic anisotropies of some chondritic meteorites. J. Geophys. Res., **66**, 1523–1534.

WALSH, J. B. and DECKER, E. R. (1966): Effect of pressure and saturating fluid on the thermal conductivity of compact rock. J. Geophys. Res., **71**, 3053–3061.

YANAI, K., comp. (1979): Catalog of Yamato Meteorites. 1st ed. Tokyo, Natl Inst. Polar Res., 188 p. with 10 pls.

YOMOGIDA, K. and MATSUI, T. (1981): Physical properties of some antarctic meteorites. Mem. Natl Inst. Polar Res., Spec. Issue, **20**, 384–394.

(Received June 1, 1982; Revised manuscript received August 24, 1982)